EPTT 2024
Escola de Primavera de Transição e Turbulência

ABCM
Associação Brasileira de Engenharia e Ciências Mecânicas

EPTT-2024-0048
SIMULATION OF THE UNSTABLE ATMOSPHERIC BOUNDARY LAYER OF AMAZON RAINFOREST USING LARGE-EDDY SIMULATION

Mateus Popoff
Livia Souza Freire
Instituto de Ciências Matemáticas e de Computação, Universidade de São Paulo, São Carlos/SP
mateuspopoff@gmail.com; liviafreire@usp.br

Resume. *Understanding the phenomena that occur in the atmospheric boundary layer (ABL) of the Amazon forest is important to deepen our knowledge about their local and global impacts. Turbulence is the main mechanism for mixing the chemical components produced within the canopy and transporting these substances from the forest surface to the top of the ABL. The Large-Eddy Simulation (LES) is a useful tool in the representation of the ABL, but it is not computationally capable of enabling a high-resolution simulation close to the surface within an extensive vertical domain. The solution proposed in this article for this problem is the use of the One-Dimensional Turbulence (ODT) wall model. When coupled to the LES, the ODT replaces the need for mesh refinement close to the ground, generating stochastic vortices that aim to replicate the turbulence statistics in this area. In this work, a simulation of the Amazon ABL is performed for two types of thermal instability, namely forced convection and free convection. Results are compared to experimental data and the behavior of the model is discussed. In general, the LES-ODT model showed satisfactory results, although some statistics could not be reproduced exactly. In the future, the coupled LES-ODT model can be used to investigate the ABL behavior in the presence of vegetation for different thermal stability conditions.*

Keywords: *Turbulence; Large-Eddy Simulation; Atmospheric Boundary Layer, Amazon Rainforest*

1. INTRODUCTION

The Amazon forest is environmentally important on local and global scales (Pachauri *et al.*, 2014) and turbulence is the phenomenon by which chemical substances are transported from its canopy to the top of the atmospheric boundary layer (ABL), influencing its rainfall regime (Fuentes *et al.*, 2016), among other physical phenomena. This project focuses on studying turbulence through the statistics of ABL flow in the region close to the forest, essential for understanding air intrusion and exhaustion events in the canopy. To achieve the objective of this work, it is necessary to simulate the unstable ABL of this forest and validate the results with experimental data obtained from the GoAmazon project (Martin *et al.*, 2017).

The simulation of unstable ABL requires an extensive vertical domain due to the increased ABL height caused by convective turbulence. In addition, the direct numerical simulation of the ABL requires extensive computational power, because the domain is in the order of kilometers while the mesh cells must be in the order of millimeters, since $Re \gtrsim 10^7$ (Feng *et al.*, 2020). One method to enable this type of simulation is with the Large-Eddy Simulation (LES) turbulence model, which allows the mesh cells to be larger by modelling the effects of small-scale turbulence. Another problem comes when the simulation has a solid surface below, because this surface will require even more refinement close to it, making the application of this kind of simulation not affordable as well (Pope, 2000). To overcome this problem, the LES must be used with wall models, and the main proposal of this project is to apply the LES coupled to the One-Dimensional Turbulence (ODT) wall model. The ODT is able to generate turbulence statistics with stochastic eddies and to detail the flow near the surface within a larger LES mesh close to the wall (Freire, 2022). This model was used before in the works of Schmidt *et al.* (2010), Kerstein *et al.* (2001), Freire (2022), Lignell *et al.* (2013), Gao *et al.* (2023) and Medina Méndez and Schmidt (2023). Also, the implementation of the model in the simulator was verified in the work of Freire (2022), having a comparison of the ODT results along with the Monin-Obukhov Similarity Theory (MOST) wall model.

To validate the simulation, field experimental data obtained during the GoAmazon project (Fuentes *et al.*, 2016) is used, and statistics of the flow under free convection and forced convection are obtained by the ratio between canopy height (h_c) and the Obukhov length (L). As suggested by Dupont and Patton (2012), for values of $0.01 < -h_c/L < 0.2$, the flow is in forced convection, and for $0.2 < -h_c/L < 20$ it is in free convection.

2. LARGE-EDDY SIMULATION

The Large-Eddy Simulation is a technique that filters the small fluctuations from a fluid flow, creating a new term called residual anisotropic stress tensor (τ_{ij}^r) on the filtered Navier-Stokes equation that represent the effects of the unresolved small scales. This term introduces new variables, for this reason it is necessary to introduce different models to make the group of four equations solvable (Pope, 2000). This work used the scale-dependent Lagrangian dynamic model, which uses temporal means through the course of the particles inside the domain to calculate this tensor value, avoiding many kinds of restrictions and errors (Bou-Zeid *et al.*, 2005). For incompressible fluids from atmospheric flows, the filtered equations of conservation of mass (continuity), momentum and the transport of potential temperature are, respectively:

$$\frac{\partial \widetilde{U}_i}{\partial x_i} = 0, \tag{1}$$

$$\frac{\partial \widetilde{U}_i}{\partial t} + \frac{\partial \widetilde{U}_i \widetilde{U}_j}{\partial x_j} = -\frac{\partial \widetilde{P}^r}{\partial x_i} + f(\widetilde{U}_2 - V_g)\delta_{i1} - f(\widetilde{U}_1 - U_g)\delta_{i2} - g\frac{\widetilde{\Theta}'}{\Theta_0}\delta_{i3} - \frac{\partial \tau_{ij}^r}{\partial x_j}, \tag{2}$$

$$\frac{\partial \widetilde{\Theta}}{\partial t} + \frac{\partial \widetilde{\Theta} \widetilde{U}_j}{\partial x_j} = -\frac{\partial}{\partial x_j}\left(-\frac{\nu_r}{Pr_r}\frac{\partial \widetilde{\Theta}}{\partial x_j}\right) = -\frac{\partial q_j}{\partial x_j}, \tag{3}$$

where $\widetilde{U}_i$ is the i component for the filtered velocity, x_i is the i component for space, t is time, $\widetilde{P}^r$ is the filtered modified pressure, f is the Coriolis parameter, U_g and V_g are the geostrophic winds, δ_{ij} is the Kronecker delta, g is the gravity, $\widetilde{\Theta}'$ is the deviation from the planar mean of the potential temperature, Θ_0 is the planar mean of the potential temperature, $\widetilde{\Theta}$ is the filtered potential temperature, ν_r is the residual viscosity, Pr_r is the sub-grid Prandtl number and q_j is the sub-grid potential temperature flux.

The temperature plays a special role in the fluids, because a hot parcel of gas is less dense than a cold one. To consider this effect for an incompressible simulation, the term $\widetilde{\Theta}'/\Theta_0$ is used in equation (2), from the Boussinesq approximation. It increases the upward velocity in case $\widetilde{\Theta}'$ is positive, and downward if negative (Freire, 2022). The potential temperature, given by Θ, is a measure that corrects for temperature modifications due to the vertical decrease in pressure, because when the parcel of air gets higher, the pressure drops and also the temperature, but the energy remains the same. Then, Θ is an important variable that allows to analyze the buoyancy effects without the need to account for the pressure on the results. Also, it is relevant to consider the Coriolis effect, as it can be seen also in equation (2) (Wallace and Hobbs, 2006).

There are three types of range of scales in turbulence, the largest is the production range, in the middle is the inertial range and the smaller one is the dissipation range. The size of the LES filter must be within the inertial range to be effective, but this range decreases in the region close to the wall. A reasonable explanation for this is because the size of the largest eddies are the distance from the surface to its center, and this size gets smaller when it gets closer to the wall. Therefore, a refinement of the mesh next to the surface is needed (which increases the computational cost), or a wall model needs to be employed (Davidson, 2015).

3. ONE-DIMENSIONAL TURBULENCE

The One-Dimensional Turbulence (ODT) model was created by Kerstein (1999) and initially used as an independent model for generation of turbulence statistics in a single line, which is the ODT domain. All the variables are independent of each other, and the main advantages of this model are the ability to represent multiple scalar fields, the capacity to model transient flows and its stochastic eddies. However, a problem is that its results can be interpreted only in terms of means, variances and high order statistics (Freire and Chamecki, 2018). The ODT was adopted in this work as a wall model coupled with LES, as it was done by Schmidt *et al.* (2003); McDermott (2005); Freire (2022). The main set of equations are filtered like LES, through a new filter in ODT scale, given by:

$$\frac{\partial \tilde{u}_i}{\partial t} + \frac{\partial \tilde{u}_i \tilde{v}_j}{\partial x_j} = f(\tilde{u}_2 - V_g)\delta_{i1} - f(\tilde{u}_1 - U_g)\delta_{i2} - \frac{\partial \tau_{i3}^*}{\partial x_3} + d_i + \textit{stochastic eddies}, \tag{4}$$

$$\frac{\partial \tilde{\theta}}{\partial t} + \frac{\partial \tilde{\theta} \tilde{v}_j}{\partial x_j} = -\frac{\partial q_3^*}{\partial x_3} + S_h + \textit{stochastic eddies}, \tag{5}$$

in which,

$$\tau_{i3}^* = -\nu_{r*}\frac{\partial \tilde{u}_i}{\partial x_3}, \qquad \text{and} \qquad q_3^* = \frac{\nu_{r*}}{Pr_r}\frac{\partial \tilde{\theta}}{\partial x_3}, \tag{6}$$

which $\tilde{u}$ is the filtered velocity resolved in ODT, $\tilde{v}$ is the LES velocity in ODT scale, τ^* is the sub-grid momentum tensor, d_i is the drag force caused by the canopy, $\tilde{\theta}$ is the potential temperature resolved in ODT, q^* is the sub-grid heat flux, S_h

is the heat source also caused by the canopy, and ν_{r*} is the sub-grid viscosity in the ODT scale (Freire, 2022). The drag term and the heat source are given by the following equations respectively:

$$d_i = -C_d \mathbf{P} a_f(x_3)|u_i|u_i, \tag{7}$$

$$S_h = \frac{\partial Q(x_3)}{\partial x_3} = \frac{\partial (Q_h \exp(-\gamma A_c))}{\partial x_3}, \qquad \text{with} \qquad A_c = \int_{x_3}^{h_c} a_f dx_3, \tag{8}$$

where C_d is the drag force coefficient, $\mathbf{P}$ is a diagonal matrix with 0.5 in its values, a_f is the Leaf Area Density (LAD), and for the other equation $Q(x_3)$ is the heat flux profile, Q_h is the heat flux at the top of the canopy, γ is a light extinction coefficient and A_c is the decreasing cumulative LAD with h_c being the canopy height. The main idea is that Q_h is the maximum heat flux for S_h, and this source gets weaker when it's closer to the surface accordingly to the LAD profile, mimicking the sunlight getting through the canopy leafs and heating the atmosphere (Nebenführ and Davidson, 2015; Gerken *et al.*, 2017).

The coupling between LES and ODT is illustrated by Figure 1, which shows that inside the LES mesh cells there is an ODT domain divided between the ODT region and ODT overlap region. In the ODT region, the flow field is driven by LES and refined by ODT, and the refined information is transferred back to the LES (two-way coupling). The overlap region solves LES equations with ODT stochastic fluxes (centered in the ODT region) added to τ_{ij}^r and q_j. In each time-step of the LES iteration, there are fifteen time-steps for ODT. The variables v_1 and v_2 are velocities in the center of the LES cell that are transferred into constants through ODT iterations. However, to guarantee the incompressibility state, v_3 is calculated using the following equation:

$$\hat{v}_3(z) = -\int_0^z \left(\frac{\partial \hat{v}_1}{\partial x_1} + \frac{\partial \hat{v}_2}{\partial x_2} \right) dz, \tag{9}$$

where z denotes a desired height.

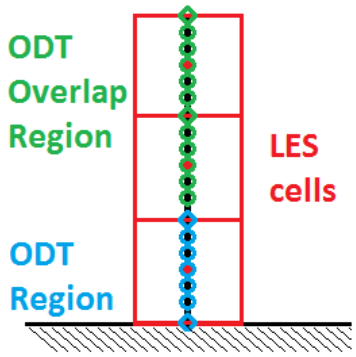

Figure 1. Scheme of LES-ODT coupling above a surface. The LES cells are represented by red squares, the ODT region is denoted by blue circles and the ODT overlap region is drawn in green circles.

The stochastic eddies are given by a specific physics-based equation, which takes into account the velocities and potential temperature, representing the energy contained in those eddies. The probability of occurrence of a stochastic eddy is given by

$$\lambda(l, z_b; t) = \frac{C_\lambda}{l^3} \sqrt{\frac{1}{3}\left(u_{1,K}^2 + u_{2,K}^2 + u_{3,K}^2 + \frac{8gl}{27}\frac{\theta_K}{\theta_0} \right)}, \tag{10}$$

where l is the size of the stochastic eddy, z_b is the bottom height of this eddy, C_λ is a constant that controls the eddies frequency and $u_{i,K}$ and θ_K are properties of velocity and potential temperature, better explained in the article of Freire and Chamecki (2018).

4. METHODS

The LES code used in this study uses a pseudo-spectral method to compute the horizontal derivatives, a second-order finite-difference method to calculate the vertical derivative and an explicit second-order Adams-Bashforth for time. The potential temperature and horizontal velocities are calculated in the center of the cells and the vertical velocity on the cells' faces (staggered in vertical). The horizontal directions are periodic, the surface at the bottom of the domain have a zero vertical velocity boundary condition and just above, in the ODT region, the canopy and its effects are considered.

The top of the domain has a stress-free boundary condition and above 1500 meters a potential temperature gradient is applied to cease the turbulence above, delimiting the ABL height (Freire, 2022).

The size of the domain is of $5888\,\mathrm{m} \times 5888\,\mathrm{m} \times 2944\,\mathrm{m}$, the number of LES cells are 64^3 and ODT cells are 48 on ODT region and 168 in the ODT overlap region. The canopy height is given by h_c and it is $36\,\mathrm{m}$. The Coriolis parameter is equal to -7.887×10^{-6} and the simulation takes 200 000 time steps with 0.1 seconds each. The streamwise velocity is initiated with a log curve, and random fluctuations are added to all three velocity components. The top region have a horizontal velocity imposed as $(Ug, Vg) = (16, 0)$, and the Q_h is given by $0.1\,\mathrm{Km/s}$ for the forced convection case and $0.5\,\mathrm{Km/s}$ for the free convection case. The LAD of the canopy is represented in Figure 2 and specifies how the drag force and the heat source will act in the simulation. Notice that the LAD's peak is around $0.6\,h_c$.

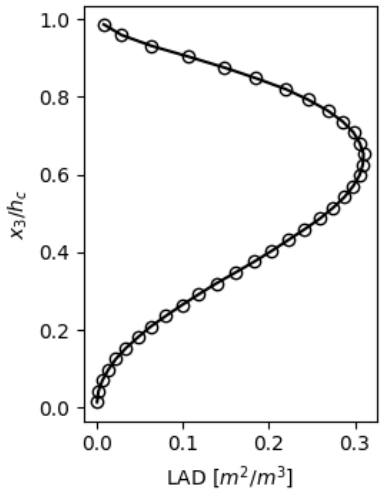

Figure 2. Leaf area density used to represent the drag force and the heat source of the canopy.

All statistics are calculated after 100 000 time-steps using the remaining 100 000 time-steps of the simulation, which gives approximately 2.78 hours of simulated data. For GoAmazon data, the postprocessing is based on Zahn *et al.* (2016). To normalize the results, the friction velocity on the top of the canopy is used, and it is given by $u_* = (-\tau_h)^{1/2}$, where τ_h is the total shear stress on the canopy top. The other normalization parameter used in this work is θ^*, which is the heat flux at canopy top, $\langle u_3'\theta' \rangle_h$, divided by u_* (Freire, 2022). The Obukhov length is also an important parameter and is given by the following equation:

$$L = -\frac{u_*^3 \theta_h}{\kappa g \langle u_3'\theta' \rangle_h}, \tag{11}$$

where θ_h is the potential temperature at canopy top, $\kappa = 0.41$ is the von Kármán constant and $g = 9.81$ is the gravity constant.

5. RESULTS

The results of the simulation in the region near the canopy are presented in Figure 3. The cases of comparisons are Qh01 (LES-ODT with $Q_h = 0.1$) compared to the GoAmazon forced-convection data (FoC), and $Q_h = 0.5$ (Qh05) compared to the GoAmazon free-convection case (FrC). For Qh01, the final ABL height is $1633\,\mathrm{m}$, and for Qh05 the final height is $1817\,\mathrm{m}$. The parameter that determine the type of atmospheric flow, $-h_c/L$, is 0.06 for Qh01 and 0.27 for Qh05, which defines these simulations as forced convection and free convection respectively. The normalization parameters for each case are presented in the Tab. 1. The region of interest in this study is the one close to the canopy, which is resolved by the ODT model.

Figure 3(a) represents the mean horizontal velocity $\bar{u}$, which has an inflection point close to the canopy top, where the LAD starts to get stronger (at $0.8\,h_c$). The maximum of the Qh05 horizontal velocity is lower than the Qh01, similar to the GoAmazon FrC compared to FoC data, because free convection flows have more upward flow and vertical mixing caused by the stronger buoyancy forces. For Qh01, this result is within one standard deviation (SD) of the field data, but Qh05 is below one SD of the field data. We note that, giving the lack of upper air information in the field data, it is not possible to match exactly the forcing of the flow with field conditions, which may explain this discrepancy. Also, the field data is biased towards stronger winds, which is when the sensors behave best. Deep inside the canopy, all results have a better match with field data, indicating the appropriate use of the LAD profile.

All the variances, showed by Figure 3(b), (c) and (d), have a drastic reduction in the deeper regions of the canopy, which indicate that there is a low turbulence kinetic energy in this region. Only the vertical variance, in (d), is significantly

Table 1. Normalization parameters for all cases. u_* is the friction velocity in m/s, θ^* is the heat flux normalization parameter in K, θ_h is the potential temperature at the canopy top in K, $\langle u_3'\theta'\rangle_h$ is the heat flux at the canopy top in Km/s, L is the Obukhov length in meters and $-h_c/L$ is the dimensionless parameter that defines the ABL state.

Case	u_*	θ^*	θ_h	$\langle u_3'\theta'\rangle_h$	$-L$	$-h_c/L$
FoC	0.6	0.102	4.39	0.061	266.668	0.135
FrC	0.438	0.204	4.067	0.09	70.582	0.51
Qh01	0.751	0.126	1.804	0.095	595.599	0.06
Qh05	0.838	0.567	7.068	0.475	134.699	0.267

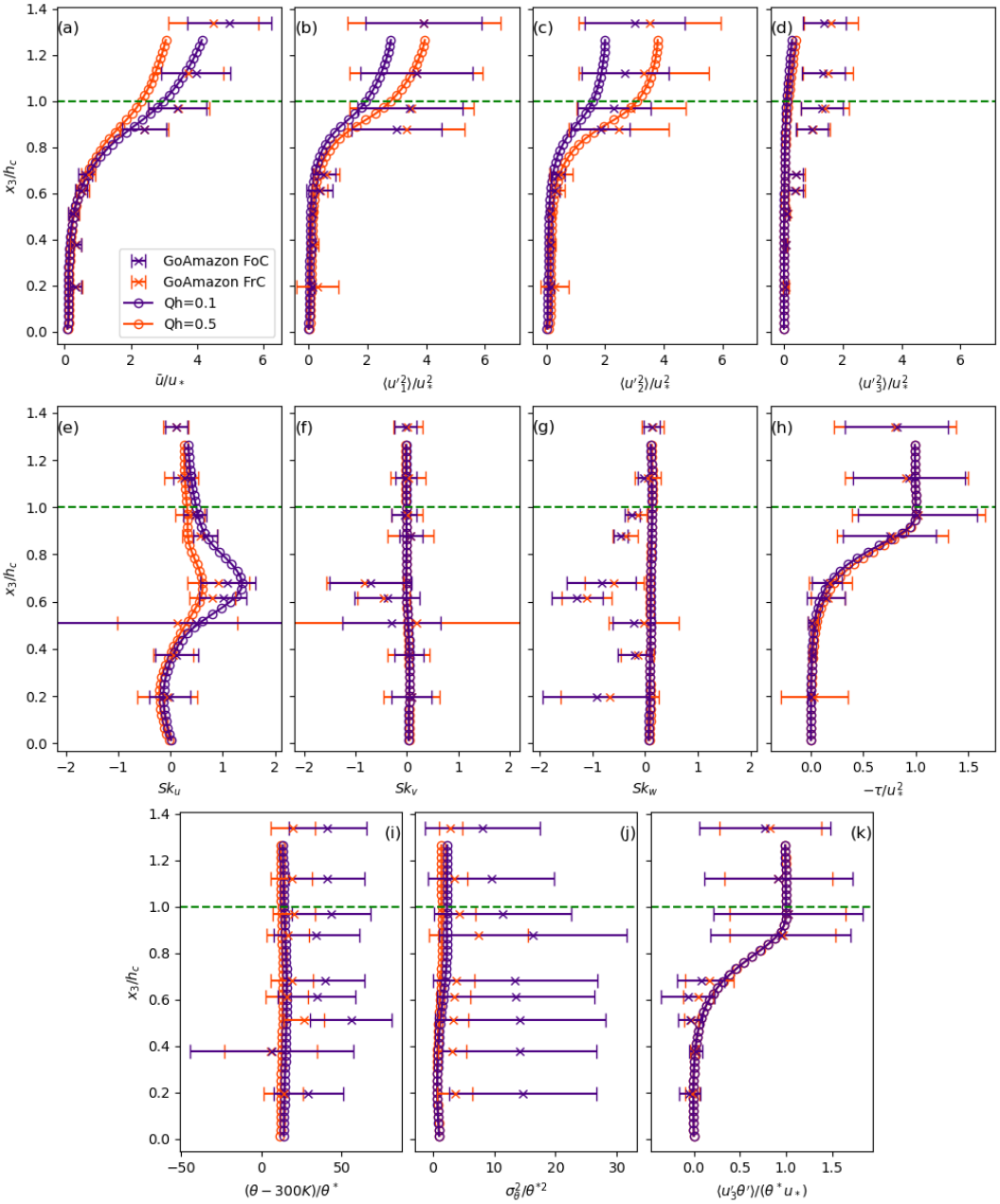

Figure 3. Statistical results in the canopy region. The green dashed line represents the canopy top, (a) is the mean horizontal velocity, (b), (c) and (d) are the velocity variances, (e), (f) and (g) are the velocity skewness, (h) is the shear stress, (i) is the potential temperature, (j) is the potential temperature variance and (k) is the heat flux.

underpredicted compared to the field data, which is an expected behavior for the ODT model (Freire and Chamecki, 2018). But for horizontal variances, in (b) and (c), the results are compatible with the GoAmazon data for both cases, with values inside the range of one SD.

Skewness results are presented in Figure 3(e), (f), and (g). This is an important result because it is a higher order statistics, which represents the sweeps and ejections inside the canopy. Only the longitudinal direction, given by Sk_u, shows a behavior different from zero, and the height of the peak from the simulation is in accordance with data results for both cases. Also, the top region of the simulated canopy is in agreement with the data, and it seems that the convection plumes enter deep in the canopy. An interesting result of this simulated statistics is that the peak is in the same high as the peak of LAD, for both cases. The other two skewnesses suggest that the ODT cannot reproduce expressive results for this kind of statistics in these directions. As expected for the data result, the vertical skewness, given by Sk_w, is negative though the canopy because these injection vortices are in a downward direction (Finnigan, 2000), but the ODT cannot reproduce this result (Freire, 2022). Therefore, the only skewness that is totally in accordance with data is Sk_u.

The shear stress in Figure 3(h) stays linear above the canopy and decreases within the canopy. This is a variable that represents the vertical transport of horizontal momentum, where more momentum is transferred from higher regions of the flow to the lower regions where the presence of the surface ceases the movement, giving a downward direction to horizontal momentum flux. Because the normalization parameter is based on this value, forcing all results to match at canopy top, the most important thing to analyze is the shape of the curve, which is in accordance with the field data for both cases. Because there is no significant amount of horizontal momentum in deeper regions of the canopy, this vertical transport also tends to decrease. Despite the fact that above the canopy region this shear stress looks constant, in an ABL point of view this variable tends to zero linearly, reaching zero at the top of the ABL (not shown).

The potential temperature result is given by Fig. 3(i), and the SD from field data is large compared to their average value. The Qh05 case shows agreement with FoC data, but the Qh01 is partially off the SD range. The variance of the potential temperature is in Fig. 3(j), and again the case is similar to the previous analysis, where the FrC is in agreement with Qh05, but the FoC case does not have not an accurate result. Finally, the heat flux result is represented in Fig. 3(k), and again this statistics was used to define the normalization parameter forcing all the curves to match at canopy top, and the shape of the curves show the simulation values inside the SD ranges given by the field data. The behavior of this heat flux is similar to the shear stress but with opposite sign, as the heat flux is upward. Again, despite the fact that above the canopy the heat flux looks constant, in an ABL point of view it is decreasing linearly until reaching zero in the top limit of the ABL (not shown).

6. CONCLUSION

For a stochastic-based model, the ODT showed assertive results when compared to the GoAmazon data, despite a few statistics with underpredicted values. For some statistics, the free convection was better represented, and others the forced convection showed better results. In the future, the skewness results must be analyzed together with the drag force diagonal matrix, $\mathbf{P}$, in order to confirm the possibility of a better representation for the vortex injections inside the canopy. The potential temperature results should also be better investigated, considering a possible bias in the field data for the mean temperature, and other forms of normalization. Because the mean horizontal velocity is in the same order of magnitude as the GoAmazon data, and their horizontal variances, shear stress and heat fluxes are in agreement, it is possible to consider that the LES-ODT model can be used to represent the convective boundary layer in the Amazon rainforest.

7. ACKNOWLEDGEMENTS

The funds of this study are from the São Paulo Research Foundation (FAPESP), grant numbers 2022/04691-6 and 2018/24284-1. Research carried out using the computational resources of the Center for Mathematical Sciences Applied to Industry (CeMEAI) funded by FAPESP (grant 2013/07375-0).

Bou-Zeid, E., Meneveau, C. and Parlange, M., 2005. "A scale-dependent lagrangian dynamic model for large eddy simulation of complex turbulent flows". *Physics of fluids*, Vol. 17, No. 2, p. 025105.

Davidson, P.A., 2015. *Turbulence: an introduction for scientists and engineers*. Oxford university press.

Dupont, S. and Patton, E.G., 2012. "Influence of stability and seasonal canopy changes on micrometeorology within and above an orchard canopy: The chats experiment". *Agricultural and forest meteorology*, Vol. 157, pp. 11–29.

Feng, S., Zheng, X., Hu, R. and Wang, P., 2020. "Large eddy simulation of high-reynolds-number atmospheric boundary layer flow with improved near-wall correction". *Applied Mathematics and Mechanics*, Vol. 41, No. 1, pp. 33–50.

Finnigan, J., 2000. "Turbulence in plant canopies". *Annual review of fluid mechanics*, Vol. 32, No. 1, pp. 519–571.

Freire, L.S., 2022. "Large-eddy simulation of the atmospheric boundary layer with near-wall resolved turbulence". *Boundary-Layer Meteorology*, Vol. 184, No. 1, pp. 25–43.

Freire, L.S. and Chamecki, M., 2018. "A one-dimensional stochastic model of turbulence within and above plant canopies". *Agricultural and Forest Meteorology*, Vol. 250, pp. 9–23.

Fuentes, J.D., Chamecki, M., Dos Santos, R.M.N., Von Randow, C., Stoy, P.C., Katul, G., Fitzjarrald, D., Manzi, A., Gerken, T., Trowbridge, A. *et al.*, 2016. "Linking meteorology, turbulence, and air chemistry in the amazon rain

forest". *Bulletin of the American Meteorological Society*, Vol. 97, No. 12, pp. 2329–2342.

Gao, T., Schmidt, H., Klein, M., Liang, J., Sun, M., Chen, C. and Guan, Q., 2023. "One-dimensional turbulence modeling of compressible flows: Ii. full compressible modification and application to shock–turbulence interaction". *Physics of Fluids*, Vol. 35, No. 3.

Gerken, T., Chamecki, M. and Fuentes, J.D., 2017. "Air-parcel residence times within forest canopies". *Boundary-Layer Meteorology*, Vol. 165, pp. 29–54.

Kerstein, A.R., 1999. "One-dimensional turbulence: model formulation and application to homogeneous turbulence, shear flows, and buoyant stratified flows". *Journal of Fluid Mechanics*, Vol. 392, pp. 277–334.

Kerstein, A.R., Ashurst, W.T., Wunsch, S. and Nilsen, V., 2001. "One-dimensional turbulence: vector formulation and application to free shear flows". *Journal of Fluid Mechanics*, Vol. 447, pp. 85–109.

Lignell, D., Kerstein, A., Sun, G. and Monson, E., 2013. "Mesh adaption for efficient multiscale implementation of one-dimensional turbulence". *Theoretical and Computational Fluid Dynamics*, Vol. 27, pp. 273–295.

Martin, S.T., Artaxo, P., Machado, L., Manzi, A.O., Souza, R.A.F., Schumacher, C., Wang, J., Biscaro, T., Brito, J., Calheiros, A., Jardine, K., Medeiros, A., Portela, B., de Sá, S.S., Adachi, K., Aiken, A.C., Albrecht, R., Alexander, L., Andreae, M.O., Barbosa, H.M.J., Buseck, P., Chand, D., Comstock, J.M., Day, D.A., Dubey, M., Fan, J., Fast, J., Fisch, G., Fortner, E., Giangrande, S., Gilles, M., Goldstein, A.H., Guenther, A., Hubbe, J., Jensen, M., Jimenez, J.L., Keutsch, F.N., Kim, S., Kuang, C., Laskin, A., McKinney, K., Mei, F., Miller, M., Nascimento, R., Pauliquevis, T., Pekour, M., Peres, J., Petäjä, T., Pöhlker, C., Pöschl, U., Rizzo, L., Schmid, B., Shilling, J.E., Dias, M.A.S., Smith, J.N., Tomlinson, J.M., Tóta, J. and Wendisch, M., 2017. "The green ocean amazon experiment (goamazon2014/5) observes pollution affecting gases, aerosols, clouds, and rainfall over the rain forest". *Bulletin of the American Meteorological Society*, Vol. 98, No. 5, pp. 981 – 997. doi:https://doi.org/10.1175/BAMS-D-15-00221.1. URL `https://journals.ametsoc.org/view/journals/bams/98/5/bams-d-15-00221.1.xml`.

McDermott, R.J., 2005. *Toward one-dimensional turbulence subgrid closure for large-eddy simulation*. The University of Utah.

Medina Méndez, J.A. and Schmidt, H., 2023. "Towards the evaluation of heat and mass transfer in pipe flows with cocurrent falling films using one-dimensional turbulence". *PAMM*, Vol. 23, No. 1, p. e202200271.

Nebenführ, B. and Davidson, L., 2015. "Large-eddy simulation study of thermally stratified canopy flow". *Boundary-layer meteorology*, Vol. 156, pp. 253–276.

Pachauri, R.K., Allen, M.R., Barros, V.R., Broome, J., Cramer, W., Christ, R., Church, J.A., Clarke, L., Dahe, Q., Dasgupta, P. *et al.*, 2014. *Climate change 2014: synthesis report. Contribution of Working Groups I, II and III to the fifth assessment report of the Intergovernmental Panel on Climate Change*. IPCC.

Pope, S.B., 2000. *Turbulent flows*. Cambridge university press.

Schmidt, R.C., Kerstein, A.R. and McDermott, R., 2010. "Odtles: A multi-scale model for 3d turbulent flow based on one-dimensional turbulence modeling". *Computer methods in applied mechanics and engineering*, Vol. 199, No. 13-16, pp. 865–880.

Schmidt, R.C., Kerstein, A.R., Wunsch, S. and Nilsen, V., 2003. "Near-wall les closure based on one-dimensional turbulence modeling". *Journal of Computational Physics*, Vol. 186, No. 1, pp. 317–355.

Wallace, J.M. and Hobbs, P.V., 2006. *Atmospheric science: an introductory survey*, Vol. 92. Elsevier.

Zahn, E., Chor, T. and Dias, N., 2016. "A simple methodology for quality control of micrometeorological datasets". *Am J Environ Eng*, Vol. 6, No. 4A, pp. 135–142.